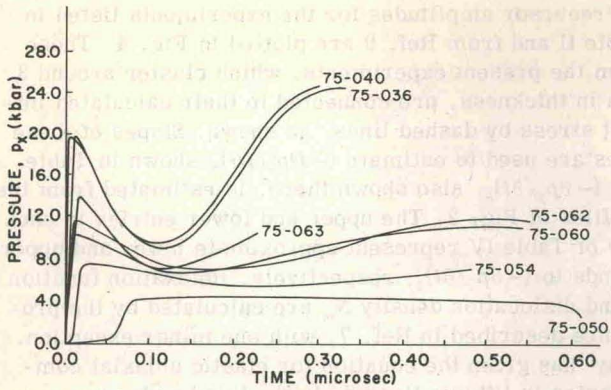

FIG. 2. Effects of impact stress on pressure-time profiles in LiF; shot numbers refer to entries in Tables II—IV.

the precursor maximum. This may arise from cross-glide multiplication of existing dislocations. Equation (5) of Ref. 9 is the constitutive relation derived for these materials. Combining this with Eqs. (2) and (13) of Ref. 7, we obtain the equation

$$\dot{N}_m = \pm \frac{3M}{C_{11} - C_{12}} \left(\dot{p}_x + \frac{C_{11}}{V} \dot{V} \right), \tag{1}$$

where $\dot{V} \equiv dV/dt$, etc., and $V = 1/\rho$ is the specific volume. The ambiguity of sign in Eq. (1) arises from the usually ignored fact that the Orowan relation, Eq. (5) of Ref. 7, involves the absolute value of the plastic strain rate. The sign in Eq. (1) is to be taken so that $\dot{N}_m$ is positive.

In Fig. 3 are shown, with exaggerated curvature, curves of uniaxial elastic compression, OAB, and curves of quasistatic uniaxial elastic-plastic compression, OANC. For a shock of final amplitude p_x^D, the locus of (p_x, V) states followed by a mass element for a steady-state shock is the sequence of two straight lines, OA and AD. For a transient condition in which the elastic precursor amplitude is at P, the locus of states from P to the final state D is bounded by curve AB and the line AD.[14] Its path, PRD, cannot be described without solving the flow equations. If PR lies along AB, $\dot{p}_x V/\dot{V} = -C_{11}$ and $\dot{N}_m$ vanishes. Since the locus PRD is not known, we cannot relate $\dot{N}_m$ to $\dot{p}_x$ directly. We can, however, obtain an upper bound for total multiplication from precursor to the minimum in p_x. Assume M, C_{11}, and C_{12} to be constant in Eq. (1) and integrate from precursor to minimum. Then

$$\Delta N_m = \pm \frac{3M}{C_{11} - C_{12}} \left[\Delta p_x + C_{11} \ln\left(\frac{V_m}{V_e} \right) \right],$$

where Δp_x and $V_m - V_e$ are changes in p_x and V over the specified interval. V_e is known from the elastic relation; V_m is not known, but it is greater than the value of V at N on the plastic compression curve. Call this V_N, then

$$\Delta N_m < - \frac{3M}{C_{11} - C_{12}} \left[\Delta p_x + C_{11} \ln\left(\frac{V_N}{V_e} \right) \right]. \tag{2}$$

Suppose that APB is a curve of constant modulus, C_{11}, and ANC is of constant modulus $K = \frac{1}{3}(C_{11} + 2C_{12})$. ANC is offset vertically from the hydrostat by $p_x^A(1 - K/C_{11})$, where p_x^A is the static HEL. Pressure on the hydrostat at volume V_e is Kp_x^e/C_{11}; therefore,

$$p_x^G = \frac{K}{C_{11}} p_x^e + p_x^A \left(1 - \frac{K}{C_{11}} \right). \tag{3}$$

Also,

$$p_x^N - p_x^G = - \int_{V_e}^{V_N} K \frac{dV}{V} = -K \ln(V_N/V_e), \tag{4}$$

and

$$\Delta p_x = p_x^N - p_x^e. \tag{5}$$

Combining Eqs. (2)—(5) gives

$$\Delta N_m < \frac{2M}{K} (p_x^N - p_x^A) < \frac{2M}{K} p_x^N. \tag{6}$$

The difference, $p_x^e - p_x^N$, does not enter explicitly into Eq. (6). This upper-limit estimate for ΔN_m depends only on the minimum in the $p_x(t)$ profile. It is evident from Fig. 2 that p_x^N does not vary by more than a factor of 2 among all the shots recorded. One would expect the number of dislocations generated by cross glide to be much greater for shot 75-040 than for shot 75-054. What probably happens is that the stress path, PRD in Fig. 3, follows the elastic curve OAB much more closely in small-amplitude shots than in large-amplitude shots. This would cause the minimum in p_x to occur at larger V, so ΔN_m is much less than the upper bound in shot 75-054; whereas in shot 75-050 the upper bound may be a reasonable estimate.

For lithium fluoride, $M \approx 3 \times 10^9/\text{cm}^2$ and $K = 698$ kbar.[15] With $p_x^N = 6$ kbar, $\Delta N_m \lesssim 1.55 \times 10^8/\text{cm}^2$. From Fig. 3 one might infer that substitution of V_N for V_m is a very bad approximation. Since the compression curves are quite straight, the errors are much smaller than the figure suggests. The value of V_m can be determined only by integrating the flow equations or by measuring the transverse component of pressure.

Shot 75-060 is the lowest amplitude one for which unambiguous decay of the precursor was recorded. Its amplitude of 10.4 kbar is 7% smaller than the calculated impact pressure of 11.2 kbar. Since resolved shear stress on the primary slip systems is 0.219 times the

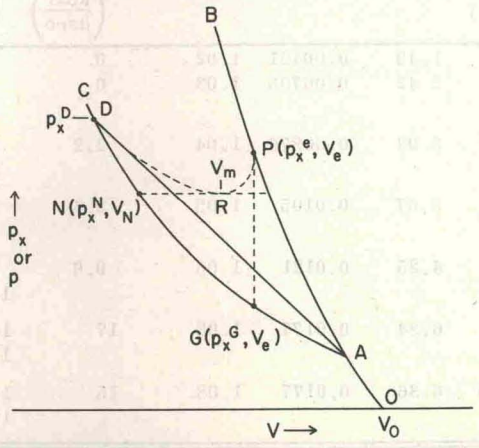

FIG. 3. Schematic representation of pressure-volume states in LiF.

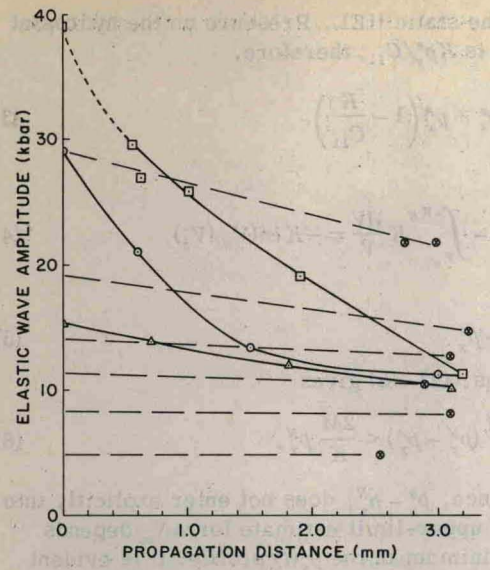

FIG. 4. Effects of impact stress and propagation distance on precursor amplitudes in LiF. ⊡, ⊙, △—measurements from Ref. 9. ⊗—new results.

impact pressure, its value is 2.4 kbar for shot 75-054 and 3.0 for shot 75-060. These numbers bound the minimum value required to nucleate dislocations around magnesium fluoride precipitates in this material, according to the model proposed in Ref. 7.

Shots 75-036 and 75-040 were intended to duplicate shot 72-015 of Ref. 9. The precursor amplitude in that case was 11.4 kbar, which is but slightly more than one-half the values obtained for shots 75-036 and 75-040. The difference may arise from a difference in magnesium concentration, discussed in Sec. III. The annealing time which is slightly shorter than Gupta's Ann. III should not produce such an effect. If surface dislocations contribute to precursor decay, such an effect might be observed due to variations in surface preparation, but experiments on this point by Asay suggest that is is not important.[5]

Precursor amplitudes for the experiments listed in Table II and from Ref. 9 are plotted in Fig. 4. Those from the present experiments, which cluster around 3 mm in thickness, are connected to their calculated impact stress by dashed lines, as shown. Slopes of these lines are used to estimate $(-Dp_x^e/Dt)$, shown in Table IV. $(-\partial p_x/\partial t)_h$, also shown there, is estimated from the profiles of Fig. 2. The upper and lower entries in each row of Table IV represent approximate lower and upper bounds to $(-\partial p_x/\partial t)_h$, respectively. Relaxation function F and dislocation density N_m are calculated by the procedure described in Ref. 7, with one minor exception. Asay[5] has given the equation for elastic uniaxial compression in lithium fluoride to the third order in strain as

$$p_x^e = C_{11}^S e(1+\alpha e), \tag{7}$$

where $e = 1-\rho_0/\rho$, C_{11}^S is an adiabatic elastic modulus, and $\alpha = 4.71$ is a dimensionless constant. With the definitions

$$C_L^2 = \left(\frac{\partial p_x^e}{\partial \rho}\right)_S \left(\frac{\rho}{\rho_0}\right)^2,$$

$$U^2 = V_0^2[p_x^e/(V_0 - V)],$$

it is readily seen from Eq. (7) that

$$C_L^2/U^2 = 1+\alpha e+0(e^2).$$

Then to the second order in e,

$$F = 2(1+\alpha e)\left(-\frac{Dp_x^e}{Dt}\right) - \alpha e\left(\frac{-\partial p_x}{\partial t}\right)_h. \tag{8}$$

Inferred dislocation density N_m is entered in the last column of Table IV. Upper and lower entries in each row show the effects of uncertainties in $(-\partial p_x/\partial t)_h$. If this derivative were set to zero, values of N_m in the last three rows would approximately double. All in all, values of N_m given in Table IV may be reliable within a factor of ~2. The principal uncertainty is probably $\bar{v}$. Even for shot 75-060, for which precursor decay is

TABLE IV. Relaxation function and dislocation parameters.

Shot No.	p_x^e (kbar)	τ^e (kbar)	e^e	C_L^2/U^2	$-\frac{Dp_x^e}{Dt}$ $\left(\frac{\text{kbar}}{\mu\text{sec}}\right)$	$-\frac{\partial p_x}{\partial t}$ $\left(\frac{\text{kbar}}{\mu\text{sec}}\right)$	F $\left(\frac{\text{kbar}}{\mu\text{sec}}\right)$	$N\bar{v}$ ($\times 10^6$/cm μsec)	D (kbar)	$\bar{v}$ $\frac{\text{cm}}{\mu\text{sec}}$	N_m (cm^{-2})
75-050	4.9	1.43	0.00421	1.02	0	0	0	...	3.63	0.0256	N_0^c
75-054	8.3	2.42	0.00705	1.03	0	4[a]	0	...	3.68	0.0715	N_0^c
						14[b]					
75-060	10.4	3.03	0.00876	1.04	2.2	22[a]	3.67	0.583	3.96	0.0888	0.657×10^7
						43[b]	2.81	0.446			0.502×10^7
75-062	12.6	3.67	0.0105	1.05	2.4	22[a]	3.95	0.625	3.77	0.117	0.534×10^7
						50[b]	2.56	0.405			0.346×10^7
75-063	14.6	4.25	0.0121	1.06	9.6	89[a]	15.2	2.41	3.96	0.129	1.87×10^7
						120[b]	13.4	2.13			1.65×10^7
75-036	21.8	6.34	0.0177	1.08	17	140[a]	25.2	4.00	3.59	0.186	2.15×10^7
						170[b]	22.7	3.59			1.93×10^7
75-040	21.85	6.36	0.0177	1.08	15	140[a]	20.8	3.31	3.68	0.184	1.80×10^7
						160[b]	19.2	3.05			1.66×10^7

[a,b] These are approximate lower and upper limits for $(-\partial p_x/\partial t)_h$.

[c] Values of dislocation density, for the unshocked material, inferred from etch pit counts are given in Table II.